How do spiral troughs form on Mars?

Jon D. Pelletier Geosciences Department, University of Arizona, 1040 East Fourth Street, Tucson, Arizona 85721, USA

ABSTRACT

A three-dimensional model for the coupled evolution of ice-surface temperature and elevation in the Martian polar ice caps is presented. The model includes (1) enhanced heat absorption on steep, dust-exposed scarps, (2) accumulation and ablation, and (3) lateral conduction of heat within the ice cap. The model equations are similar to classic equations for excitable media, including nerve fibers and chemical oscillators. In two dimensions, a small zone of initial melting in the model develops into a train of poleward-migrating troughs with widths similar to those observed on Mars. Starting from random initial conditions, the three-dimensional model reproduces spiral waves very similar to those in the north polar ice cap, including secondary features such as gull-wing–shaped troughs, bifurcations, and terminations. These results suggest that eolian processes and ice flow may not control trough morphology.

Keywords: Mars, polar, ice cap, ablation, spiral trough.

INTRODUCTION

Howard (1978) proposed that the spiral troughs of Mars form with an instability in which the ice-surface temperatures of steep, equator-facing slopes exceed 0 °C during the summer, melting the ice locally to form steeper, lower-albedo scarps (through exposure of subsurface dust-rich layers) in a self-enhancing feedback. In this model, some of the water vapor released from the equator-facing scarp may accumulate on the pole-facing slope to form a self-sustaining, poleward-migrating topographic wave. The relationship between this model and the spiral morphology of troughs has not been fully established, but Fisher (1993) introduced an asymmetric ice-velocity field into Howard's model and obtained spiral forms. Recent observations from the Mars Global Surveyor, however, suggest that ice flow near the troughs is not significant (Howard, 2000; Kolb and Tanaka, 2001), and it remains unclear precisely how the spirals form and what controls their spacing, orientation, and curvature.

In order to establish a clear link between process and form for the spiral troughs, I have constructed a three-dimensional model for trough initiation and evolution. The model is based on the processes in Howard's migrating-scarp model and includes the simplest mathematical descriptions of these processes in order to determine the necessary conditions for realistic spiral troughs. Lateral heat conduction is also included in the model, and this element is crucial for obtaining realistic troughs. The model does not include wind erosion or ice flow. The equations are similar to those from the field of excitable media, in which solitary and spiral waves resulting from the dynamics of two interacting variables have been studied in detail.

MODEL DESCRIPTION

The model equations consist of two coupled, scaled equations for the deviation of local ice-surface temperature, T, from its equilibrium value (the temperature at which no accumulation or ablation takes place), and the depth of local ice-surface topography, h, below its equilibrium value (i.e., troughs have positive h). The model includes three processes: lateral heat conduction,

$$\frac{\partial T}{\partial T} = \kappa \nabla^2 T; \quad (1)$$

accumulation and ablation,

$$\frac{\partial h}{\partial t} = \frac{1}{\tau_f} T; \quad (2)$$

and heat absorption on sun-facing, dust-exposed scarps,

$$\frac{\partial T}{\partial t} = f(T, h), \quad (3)$$

where

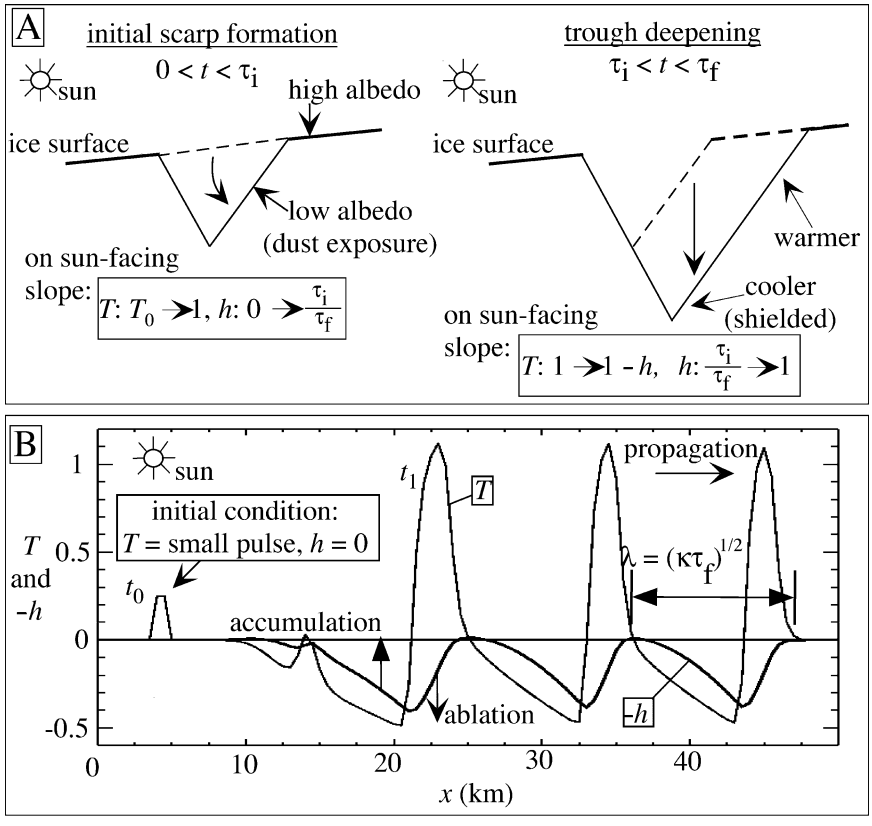

Figure 1. Diagram of trough evolution and solution to equations (see text) in two dimensions. A: Trough initiation involves rapid increase in ice-surface temperature to its maximum value as scarp is steepened and dust layers are exposed. During trough deepening, value of h steadily increases to its maximum value over time scale $\tau_f \approx 5$ m.y., while temperature decreases in deeper parts of trough due to topographic shielding. Note that $-h$ is plotted instead of h in order to show actual topographic shape (h refers to trough depth, $-h$ refers to elevation). B: Solution to equations (see text), using Runga-Kutta integration, with $\kappa = 175$ km^2, $\tau_i = 0.05$, $\tau_f = 1$, and $T_0 = 0.2$. Initial condition is small pulse with $T > T_0$ at left side of domain. Solution at $t_1 = 8$ is shown with three well-defined troughs.

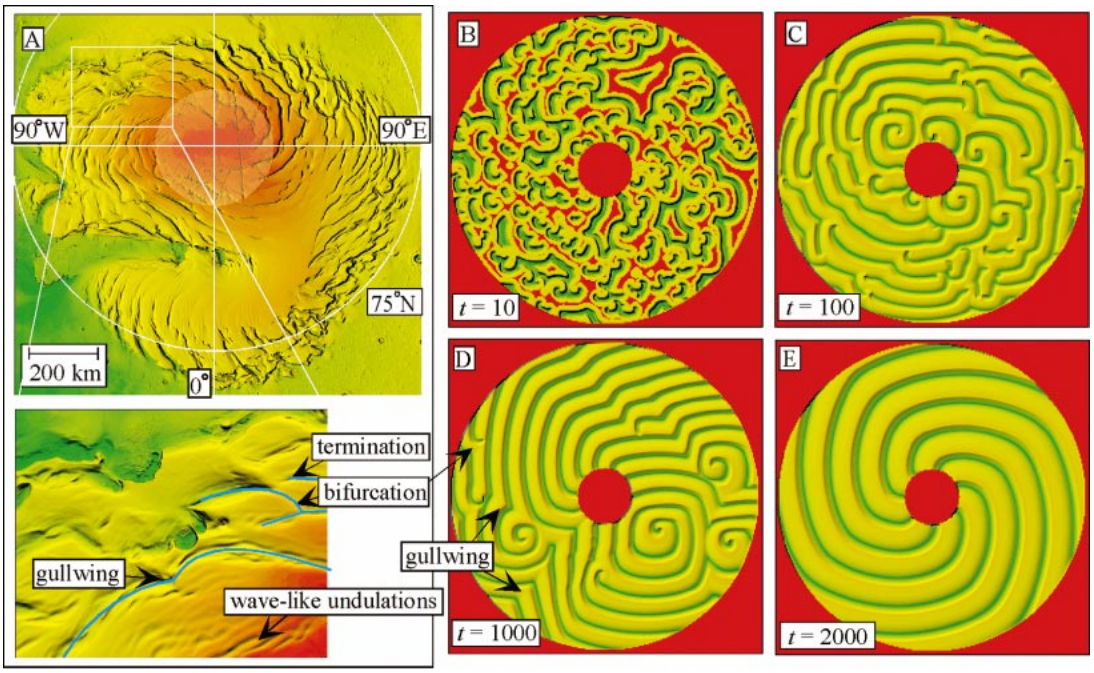

Figure 2. Numerical model results and north-polar topography. A: Shaded-relief image of Martian north-polar ice-cap digital elevation model (DEM) constructed by using Mars Orbiter Laser Altimeter topography. White region north of 88°N indicates region with DEM artifacts. Large-scale close-up indicates examples of gull-wing-shaped troughs, bifurcations, and terminations. Highest elevations are red and lowest elevations are green. B–E: Shaded-relief images of model topography, $-h$, for (B) $t = 10$, (C) $t = 100$, (D) $t = 1000$, and (E) $t = 2000$ starting from random initial conditions. Model parameters are $L = 100$ (length and width of grid, in nondimensional units), $\kappa = 0.3$, $\tau_i = 0.05$, $\tau_f = 1$ (see text). Model evolution is characterized by spiral merging and alignment in equator-facing direction. Steady state is eventually reached, as shown in E, with uniformly rotating spirals oriented clockwise or counterclockwise depending on random initial conditions.

$$f(T, h) = \frac{1}{\tau_i}[T(T - T_0)(1 - T) - h] \quad (4)$$

if

$$\nabla h \times \hat{r} \geq 0, \quad (5)$$

and

$$f(T, h) = -\frac{1}{\tau_i}h \quad (6)$$

if

$$\nabla h \times \hat{r} < 0. \quad (7)$$

In the equations, κ is the thermal diffusivity of ice, τ_i and τ_f are the time scales for initial and final scarp formation, respectively (described below), T_0 is the threshold temperature for melting, and $\hat{r}$ is the radial unit vector away from the pole. The model does not include diurnal or annual cycles; these are assumed to be included in the equilibrium temperature. Deviations from the equilibrium temperature initiate ablation and accumulation at any time, t, in the model, although accumulation and ablation of water ice on Mars are understood to be restricted to the summer months.

The initiation and deepening of troughs is assumed to take place in two steps, illustrated in Figure 1A, and controlled by the two time scales τ_i and τ_f in the model. In the first step, slope steepening and dust exposure are initiated from an undissected ice surface through a positive feedback involving ice-surface temperature, slope gradient, and albedo. In this step, the ice-surface temperature is assumed to increase from its threshold value for melting, T_0, to a maximum value of 1 over a time scale τ_i. This instability is represented mathematically in the term $f(T, h)$ by a cubic polynomial that generates a negative feedback if T is below the melting temperature, T_0, and a positive feedback for larger temperatures, bounded by a maximum value of 1. This dynamical behavior represents the triggering of melting at a threshold temperature and the positive feedback between ablation, slope gradient, and albedo as the scarp is formed. In the second step, the temperature remains near its maximum value of 1 as the trough deepens over a longer time scale, τ_f. Trough deepening does not continue indefinitely, however, because deep portions of equator-facing scarps do not absorb as much solar energy as shallow portions due to partial shielding from the pole-facing slope. The heat-absorption term $f(T, h)$ includes a term, $-h$, to represent this negative feedback. As the trough deepens and h increases in value, the temperature eventually falls below the melting temperature and accumulation begins, eventually returning the ice surface to its equilibrium elevation. The cubic term in $f(T, h)$ applies only to equator-facing slopes (i.e., $\nabla h \times \hat{r} \geq 0$).

The equations include four parameters: κ, τ_i, τ_f, and T_0. The thermal diffusivity of ice is $\kappa = 35$ m^2/yr. To estimate the vertical ablation rate on sun-facing slopes, Howard (1978) used Viking observations of summer atmospheric water-vapor concentration to obtain 10^{-4} m/yr, implying $\tau_f \approx 5$ m.y. for an average trough of 500 m depth. The time of scarp initiation is uncertain, but may be small compared with trough deepening. Here I assume that $\tau_i = 0.05\tau_f = 0.25$ m.y., which implies that ~25 m of ablation must occur before the incipient scarp is sufficiently steepened for subsurface dust to be exposed and the maximum ice-surface temperature to be reached. The model behavior is not sensitive to the precise value of τ_i as long as it is small compared with τ_f. The threshold temperature for melting, relative to the equilibrium and maximum temperatures, is between 0 and 1 and varies as a function of latitude. At 75° latitude, the maximum summer temperature of a nearly flat, high-albedo slope is ~−10 °C (Howard, 1978). The temperature difference between equator-facing troughs and nearby flats is ~40 °C (Howard, 1978). If these values are used, T_0, or 0 °C, is equal to 0.2. I assume in the model that this value applies to the entire ice cap for simplicity. The equations can be further simplified by scaling time to the value of τ_f. With this rescaling, the model is reduced to three independent parameters: $\kappa = 175$ km^2, $\tau_i = 0.05$, and $T_0 = 0.2$.

The equations herein, without the directional dependence in the term $f(T, h)$ are one example of the FitzHugh-Nagumo (FHN) equations, well-studied equations that describe excitable media. Examples of excitable media to which the FHN equations have been applied include predator-prey systems (Murray, 1989), electrochemical conduction in the heart (Winfree, 1987), chemical oscillators (Fife, 1976), and electrical transmission lines (Nagumo et al., 1965). The FHN equations come in several forms that all reproduce solitary waves in two dimensions [i.e., $h(x)$] and spiral waves in three dimensions [$h(x,y)$] for an ap-

propriate range of parameter values. Excitable media are composed of two variables: an ''activator'' (T in the equations) and an ''inhibitor'' (h in the equations). Triggering or excitation of the medium occurs when a positive feedback is initiated above a threshold value of the activator. On Mars, this process is the feedback between ablation, slope gradient, and albedo that occurs above 0 °C. Local triggering may initiate the triggering of adjacent zones through diffusive spreading of the activator (i.e., diffusion of heat laterally through the ice cap). The value of the inhibitor increases during excitation and eventually returns the system to the unexcited state through the negative coupling between h and T in the equations. On Mars this process is the topographic shielding of deep portions of the equator-facing scarp by the pole-facing slope. The FHN equations exhibit both excitable behavior, characterized by wide swings in h and T when $\tau_i \ll \tau_f$, and oscillatory behavior, characterized by smaller fluctuations when $\tau_i \approx \tau_f$ (Gong and Christini, 2003). Although both regimes may have application to Mars, here I focus on the excitable regime.

MODEL RESULTS

The solution of the equations in two dimensions is given in Figure 1B, starting with a narrow pulse of localized melting on the left side of the domain ($T = 0.25$ in the pulse, $T = 0$ elsewhere). The pulse initiates a self-sustaining train of solitary waves that propagate from left to right with the trough wave trailing the temperature wave. The width of the troughs is given by $\lambda \approx \sqrt{\kappa\tau_f}$, or 13 km for the parameters characterizing the Martian polar ice caps. This value is in good agreement with observed trough widths on Mars (Zuber et al., 1998). This behavior contrasts with that of previous models, in which troughs widened indefinitely without reaching a steady state. Another similarity with the observed topography of spiral troughs is trough asymmetry: both in the model and on Mars, equator-facing scarps are about twice as steep as pole-facing scarps (Zuber et al., 1998).

Spiral formation in equations 1–4 and 6 is illustrated in Figures 2B–2E for an idealized circular ice cap with a permanently frozen region near the pole and starting from random initial conditions. A shaded-relief image of a polar-stereographic digital elevation model (DEM) of Mars Orbiter Laser Altimeter (MOLA) data (Smith et al., 2003) is given in Figure 2A for comparison with the model results. Random initial conditions were chosen for this paper to illustrate how spirals self-organize in this system from structureless initial conditions; the actual initial conditions on Mars are unknown but may have been far from random. In these calculations I used the Barkley (1991) approximation to equation 1, which uses a semi-implicit algorithm to integrate the term $f(T, h)$ in order to gain computational speed. This Barkley (1991) algorithm enables spiral evolution to be investigated over long time scales. The early-time evolution of the model is characterized by the initiation, growth, and merging of spirals. It should be noted that heat conduction in the neighborhood of an equator-facing scarp may initiate melting in nearby regions, even if those regions face away from the equator. The late-time evolution of the model is characterized by continued spiral merging, alignment of troughs to face the equator, and a gradual increase in trough spacing as ''defects'' are removed from the system. Mature spirals face the equator at low latitudes, but curve toward the pole at higher latitudes, just as those on Mars. In the model, this poleward orientation evolves as part of the development of steady-state, rigidly rotating spiral forms. By developing poleward orientations, high-latitude scarps face perpendicular to the equator, thereby reducing ablation rates and migration speeds. Decreased migration speed offsets the smaller distance required for high-latitude scarps to complete a revolution, enabling spirals to rotate rigidly and preserve their steady-state form. The model also reproduces a number of secondary features of polar troughs on Mars, including gull-wing–shaped troughs, bifurcations, and terminations (Figs. 2A, 2C, and 2D).

The steady state of the model after $t = 2000$ is a set of seven rigidly rotating spirals. The sense of spiral orientation has an equal probability of being clockwise or counterclockwise in the model, depending on the random-number seed used to generate the initial conditions. The spiral orientation of Figure 2E is opposite to the orientation of the spirals around the north pole of Mars, but 50% of the random initial conditions I constructed for the model lead to spirals that rotate in the same sense as those on Mars (i.e., clockwise away from the pole). This behavior suggests that a uniform sense of spiraling need not represent an asymmetrical process of trough evolution. Instead, it could be the result of a minor asymmetry in the initial pattern of melting, as in the model.

DISCUSSION AND CONCLUSIONS

Several recent studies have argued that wind erosion and ice flow exert a significant control on trough morphology. Howard (2000), for example, proposed that the correlation between wind directions and trough orientations at high latitudes is the result of eolian processes. In addition, Howard (2000) argued that certain secondary features of the spiral troughs, including gull-wing shapes, provide further evidence for eolian control. The model troughs of this paper, however, reproduce poleward orientations and gull-wing shapes, even though no eolian processes are present in the model. This result suggests that eolian processes may not control trough morphology, although eolian and/or mass-movement processes must certainly be present in order to transport dust from the scarp (Howard, 2000). The agreement between observed and modeled troughs also suggests that ice flow is not required to generate realistic spiral forms. Instead, Howard's original scarp-migration model, augmented by lateral diffusion, is sufficient to reproduce the basic features of the polar troughs.

REFERENCES CITED

Barkley, D., 1991, A model for fast computer simulation of waves in excitable media: Physica D, v. 49, p. 61–70.

Fife, P.G., 1976, Pattern formation in reacting and diffusing systems: Journal of Chemical Physics, v. 64, p. 554–564.

Fisher, D.A., 1993, If Martian ice caps flow: Ablation mechanisms and appearance: Icarus, v. 105, p. 501–511.

Gong, Y., and Christini, D.J., 2003, Antispiral waves in reaction-diffusion systems: Physical Review Letters, v. 90, article 088302.

Howard, A.D., 1978, Origin of the stepped topography of the Martian poles: Icarus, v. 84, p. 2581–2599.

Howard, A.D., 2000, The role of eolian processes in forming the surface features of the Martian polar layered deposits: Icarus, v. 144, p. 267–288.

Kolb, E.J., and Tanaka, K.L., 2001, Geologic history of the polar regions of Mars based on Mars Global Surveyor data: Icarus, v. 154, p. 22–39.

Murray, J.D., 1989, Mathematical biology: New York, Springer-Verlag, 767 p.

Nagumo, J., Yoshizawa, S., and Arimoto, S., 1965, Bistable transmission lines: IEEE Transactions on Circuit Theory, v. 12, p. 400–412.

Smith, D., Neumann, G., Arvidson, R.E., Guiness, E.A., and Slavney, S., 2003, Mars Global Surveyor Laser Altimeter Mission Experiment Gridded Data Record: NASA Planetary Data System, MGS-M-MOLA-5-MEGDR-L3-V1.0.

Winfree, A.T., 1987, When time breaks down: The three-dimensional dynamics of electrochemical waves and cardiac arrythmias: Princeton, New Jersey, Princeton University Press, 339 p.

Zuber, M.T., Smith, D.E., Solomon, S.C., Abshire, J.B., Afzal, R.S., Aharonson, O., Fishbaugh, K., Ford, P.G., Frey, H.V., Garvin, J.B., Head, J.W., Ivanov, A.B., Johnson, C.L., Muhleman, D.O., Neumann, G.A., Pettengill, G.H., Phillips, R.J., Sun, X., Zwally, H.J., Banerdt, W.B., and Duxbury, T.C., 1998, Observations of the north polar region of Mars from the Mars Orbiter Laser Altimeter: Science, v. 282, p. 2053–2060.

Manuscript received 21 September 2003
Revised manuscript received 14 December 2003
Manuscript accepted 17 December 2003

Printed in USA

CORRECTION

How do spiral troughs form on Mars?: Correction

Jon D. Pelletier

Geology, v. 32, p. 365–367 (April 2004)

Several errors appear in the text of this article. They are:

Equation 1 should read

$$\frac{\partial T}{\partial t} = \kappa \nabla^2 T, \quad (1)$$

rather than

$$\frac{\partial T}{\partial T} = \kappa \nabla^2 T, \quad (1)$$

The cross product should be a dot product everywhere it appears (equations 5 and 7 and in the text). For example, equation 5 should read

$$\nabla h \cdot \hat{r} \geq 0 \quad (5)$$

instead of

$$\nabla h \times \hat{r} \geq 0 \quad (5)$$

Two additional errors were made in the manuscript text. First, the Barkley (1991) approximation was applied to equation 4, not to equation 1 as stated. Second, the term melting was incorrectly used to refer to the ablation process of the ice cap. Sublimation is the correct term.